Accepted Manuscript

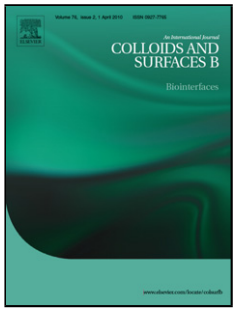

Title: A novel and ultrasensitive electrochemical DNA biosensor based on an ice crystals-like gold nanostructure for the detection of *Enterococcus faecalis* gene sequence

Authors: R. Nazari-Vanani, N. Sattarahmady, H. Yadegari, H. Heli

PII: S0927-7765(18)30169-3
DOI: https://doi.org/10.1016/j.colsurfb.2018.03.025
Reference: COLSUB 9226

To appear in: *Colloids and Surfaces B: Biointerfaces*

Received date: 13-1-2018
Revised date: 22-2-2018
Accepted date: 18-3-2018

Please cite this article as: R.Nazari-Vanani, N.Sattarahmady, H.Yadegari, H.Heli, A novel and ultrasensitive electrochemical DNA biosensor based on an ice crystals-like gold nanostructure for the detection of Enterococcus faecalis gene sequence, Colloids and Surfaces B: Biointerfaces https://doi.org/10.1016/j.colsurfb.2018.03.025

A novel and ultrasensitive electrochemical DNA biosensor based on an ice crystals-like gold nanostructure for the detection of *Enterococcus faecalis* gene sequence

R. Nazari-Vanani[1], N. Sattarahmady[1,2], H. Yadegari[3], H. Heli[1,*]

[1]Nanomedicine and Nanobiology Research Center, Shiraz University of Medical Sciences, Shiraz, Iran

[2]Department of Medical Physics, School of Medicine, Shiraz University of Medical Sciences, Shiraz, Iran

[3]Department of Mechanical and Materials Engineering, University of Western Ontario, London, Ontario N6A 5B9, Canada

[*]Corresponding author. E-mail: heli@sums.ac.ir , hheli7@yahoo.com (H. Heli)

Graphical abstract

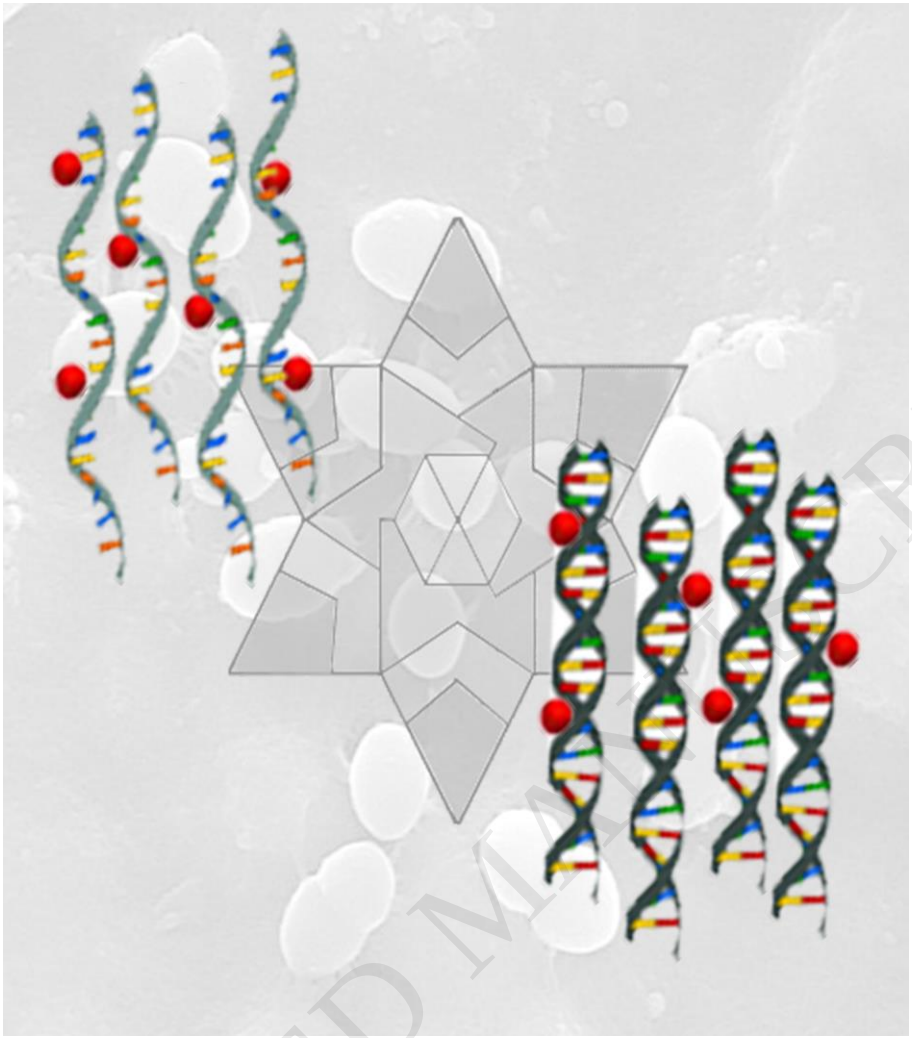

Highlights

- Ice crystals-like gold nanostructure was electrochemically synthesized.
- The gold nanostructure was employed to fabricate an *Enterococcus faecalis* genosensor.
- Toluidine blue was utilized as a hybridization redox marker.
- *Enterococcus faecalis* was detected in clinical samples.

Abstract

Bacteria, parasites and viruses are found widely in the environment as potential pathogens, and can be the source of infections. Therefore, sensitive and rapid methods for identification of the pathogens are required to achieve a better quality of life. *Enterococcus faecalis* commonly colonizes and threatens human

health. In the present study, we demonstrate the fabrication of a novel electrochemical DNA biosensor based on electrodeposited gold nanostructures as a transducer substrate combined with toluidine blue (TB) as a redox marker. Binding of TB with the single and double stranded DNA (ssDNA and dsDNA) was shortly investigated, and based on the results, TB could discriminate between ssDNA and dsDNA. A specific thiolated ssDNA sequence was immobilized on the transducer substrate, and DNA hybridization was followed by differential pulse voltammetry. The DNA biosensor showed excellent performances with high sensitivity and good selectivity. The DNA biosensor was applied to detect a synthetic target in a linear range of 1.0×10^{-17} to 1.0×10^{-10} mol L^{-1} with a limit of detection (LOD) of 4.7×10^{-20} mol L^{-1}. In addition, LOD of the DNA biosensor for the detection of genomic DNA was found to be 30.1 ng μL^{-1}.

Keywords: E. faecalis; Pathogen; Genosensor; Electrochemical biosensor

1. Introduction

Some of the bacteria, viruses and parasites are potential pathogens and hence can be a source of infection and sepsis. Therefore, detection of the pathogenic bacteria is a key step toward preventing problems related to the human's health and safety [1]. Traditional detection methods of these pathogens include cell culture, complement fixation and recently, real-time polymerase chain reaction (PCR). However, these methods generally involve labor-intensive laboratory procedures and often require trained personnel to carry them out [2]. For example, the PCR method is extremely sensitive and requires pure samples and hours of processing as well as expertise in molecular biology. Due to these problems, considerable efforts are now directed

towards the development of methods that enables the rapid detection of low concentrations of pathogens in water, food and clinical samples. Thus, biosensors have been considered as a promising approach in this regard [3-14].

Biosensors possess many unique features that make them very attractive alternative to conventional assay methods, such as their compact size, needing minimal size and preparation of sample, quick analysis, high sensitivity, accuracy, precision, specificity, reproducibility and robustness, wide detection capacity, near real-time assay, ease of use and as well as a large linear dynamic range with relatively low-cost instrumentation [3-14]. Nevertheless, the successful design and development of biosensors requires the involvement and combinations of different disciplines to achieve the desired characteristics including selectivity and sensitivity for the biological components) [3-15].

The enterococci are a diverse and versatile group of bacteria with several intrinsic characteristics that allow them to survive and grow under a variety of conditions [16]. They are Gram-positive, catalase-negative, non-spore-forming, and facultative anaerobic bacteria [17] with the ability to grow in the presence or absence of oxygen [18]. *Enterococcus* species live in the human intestinal lumen and female genital tracts and oral cavity in lesser numbers, causing no harm to their hosts under most circumstances cause no harm to their hosts [19]. However, the enterococci, especially *Enterococcus faecalis* (EF), can act as agents of infections, particularly in elderly patients with serious underlying diseases and other immunocompromised patients who have been hospitalized for prolonged periods, treated with invasive devices, and/or have received broad-spectrum antimicrobial therapy [16]. EF is the most

common nosocomial infectious agent and causes bacteremia, endocarditis, bacterial meningitis, urinary tract as well as wound infections (mostly surgical, decubitus ulcers and burn wounds) and various other infections in humankind [20, 21]. The rapid spread of EF with resistance to antibiotic has been of particular concern, and therefore its detection is important [22].

Several biosensors have been developed in the last two decades for detection of the pathogens like *Escherichia coli O157:H7* [23], *Bacillus subtilis* [24], *Salmonella* [25], influenza [7], *Brucella* [6, 8, 26] and *Leishmania* [4, 9, 10] have been performed. The major detection mechanisms of the biosensors include antibody-antigen interactions (immunosensing) [27], DNA-DNA hybridization (genosensing) [4, 7-9, 10, 26], DNA/RNA-protein interactions (aptasensing) [11, 14], and detection of pathogen biomarkers [28]. Development of DNA biosensors (genosensors and aptasensors) has received considerable attentions for applications in clinical diagnostics [7, 12, 13], and gene [29] and forensic analyses [30]. Design of the recognition elements in these genosensors is being perused to fabricate long-life, reproducible and reusable devices with enhanced specificity by affecting DNA hybridization events [7-10, 12]. As for the signal transduction route, a variety of methods of optical [4, 6, 26], piezoelectric [31] and electrochemical [7, 10, 11, 14] have been employed. Electrochemical detection techniques deliver multiple advantages including high sensitivity, capability of miniaturization, quick analysis and low-cost instrumentation [7, 10, 11, 13, 14]. Electrochemical detection methods are generally based on intrinsic redox activity of the nucleic acids [32], as well as a redox marker with direct [7, 8, 10, 11] or indirect (incorporated marker) [14] detections.

In the literature, Wang *et al.* developed an assay for visual and multiplex detection of EF in which differentiation of the EF-specific gene was accomplished using fluorescein (FITC)-and digoxin-modified primers in a multiple loop-mediated isothermal amplification process (LAMP) [33]. In the presence of biotin- and FITC-/digoxin- modified primers, the multiple LAMP yielded numerous biotin- and FITC-/digoxin- attached duplex products which were detected by lateral flow biosensor (LFB) through biotin/streptavidin interaction and immunoreactions. The accumulation of gold nanoparticles generated a characteristic red line, enabling visual and multiplex detection of target pathogens. The limit of detection of the LAMP-LFB method for detecting the EF-specific gene was 250 fg per reaction. In another study, two bioluminescence-based reporter systems for the direct detection of the quorum-sensing regulated expression of the gelatinase biosynthesis-activating pheromone (GBAP) and the cytolysin small subunit (CylL(S)) in natural samples were constructed [34]. The two EF reporters conditionally expressed bioluminescence in the presence of GBAP and CylL(S) in three hours with high sensitivity. Clavanin A peptide and cysteine-modified gold nanoparticles were also employed for the development of a sensitive biosensor for EF detection in a concentration range of 10 to 10^4 CFU [35].

In this study, we report the fabrication of an ultrasensitive electrochemical DNA biosensor for EF genome. A new nanostructure of ice crystals-like of gold as a transducer substrate, a novel DNA sequence as a probe, and toluidine blue (TB) as a novel DNA hybridization indicator were employed for a rapid and simple detection route for EF in human samples.

2. Experimental section

2.1. Chemicals

All chemicals were purchased from Scharlau (Spain) or Sigma (USA) and were used without further purification. All solutions were prepared using redistilled water. All DNA oligonucleotide sequences were obtained from Takapouzist Co. (Iran). The nucleotide sequences were as follows:

Probe DNA (p-DNA) sequence:

5' SH-TTTTTTTTTTCAATTGGAAAGAGGAGTGGCGGACG 3'

Complementary DNA (c-DNA) sequence:

5' CGTCCGCCACTCCTCTTTCCAATTG 3'

Non-complementary DNA (nc-DNA) sequence:

5' CAGAATTTCAGAAGACCCAAACGAT 3'

One base mismatched complementary DNA (1miss-DNA) sequence:

5' CGTCCGCCACTCCTCTTTCTAATTG 3'

Two base mismatched complementary DNA (2miss-DNA) sequence:

5' CGTCCGCCACTCCTCTTTATAATTG 3'

Three base mismatched complementary DNA (3miss-DNA) sequence:

5' CGTCCGCCACTCCTATTTATAATTG 3'

Forward PCR primer:

5' CGCTTCTTTCCTCCCGAGT 3'

Reverse PCR primer:

5' GCCATGCGGCATAAACTG 3'

All these oligonucleotides were dissolved in 20 mmol L^{-1} Tris-HCl buffer, pH 7.4 solution (Tris), aliquot into smaller volumes and stored at -20 °C.

2.2. Instrumentation

A μ-Autolab potentiostat/galvanostat (the Netherlands) controlled by the GPES software was used for all electrochemical experiments in a three-electrode setup using a gold disk (Au) electrode with 2 mm of diameter covered with the ice crystals-like gold nanostructure (Au/nano) was employed as the working electrode. A platinum wire and an Ag/AgCl saturated KCl were applied as counter and reference electrodes, respectively. Differential pulse voltammograms (DPVs) were recorded with a pulse width of 25 mV, a pulse time of 50 ms, and a scan rate of 10 mV s^{-1}. PCR was carried out in a thermal cycler of Bio-Rad T100 (USA). The concentrations of DNA samples were measured by a NanoDrop™ Lite Spectrophotometer (USA).

2.3. Preparation of the electrodes and electrolytes

The Au electrode was polished with alumina powder of 0.05 μm to reach a mirror-like surface before covering with the ice crystals-like gold nanostructure. Then the electrode was ultrasonically treated in an ethanol/water 3:1 (v/v) mixture for a few minutes and rinsed with redistilled water.

A ferricyanide/ferrocyanide solution containing 0.5 mol L^{-1} KCl and 0.5 mmol L^{-1} $K_4Fe(CN)_6/K_3Fe(CN)_6$ (1:1) were prepared for the electrochemical measurement of the microscopic surface areas of the working electrodes. Piranha solution was prepared by mixing hydrogen peroxide and concentrated sulfuric acid in a 1:2 (v/v) ratio. It was prepared immediately prior to use to maintain its reactivity. A stock of solution of 20 μmol L^{-1} TB was prepared in Tris and employed as redox indicator for revealing DNA hybridization. All the above solutions were kept at -4 °C before use. Dithiothreitol (DTT) solution containing 10 mmol L^{-1} sodium acetate and 500 mmol L^{-1} DTT , pH 5.2 was prepared and kept at -20 °C.

2.4. Surface area measurement

The microscopic surface area of the Au/nano electrode was electrochemically measured. The electrode was soaked in the ferricyanide/ferrocyanide solution and cyclic voltammograms at different potential sweep rates ranging from 5 to 300 mV s^{-1} were recorded. In the voltammograms, the dependency of the peak current on the potential sweep rate is [36]:

$$I_p = (2.69\times10^5)n^{3/2}AC^*D^{1/2}\nu^{1/2} \quad (1)$$

where I_p, n, A, C^*, D and ν are the peak current, number of exchanged electrons, real surface area, bulk concentration, diffusion coefficient, and potential sweep rate, respectively. For the ferricyanide/ferrocyanide redox transition, n=1, and $D=7.60\times10^{-6}$ cm s^{-1} [37].

2.5 Electrodeposition of the ice crystals-like gold nanostructure and physicochemical characterizations

For preparation of the Au/nano electrode, the Au electrode was placed in a synthesis solution comprising 0.5 mol L^{-1} H_2SO_4, 20 mmol L^{-1} $HAuCl_4$ and 150 mmol L^{-1} sorbitol. Electrodeposition was performed at 0.0 V for 300 s followed by washing the electrode surface with redistilled water and drying at room temperature. To survey the surface morphology, field emission scanning electron microscopy (FESEM) at different magnifications was applied by a TESCAN Mira 3-XMU (Czech Republic) equipped with energy-dispersive X-ray spectroscopy (EDS). The fractal dimension of the gray-scale FESEM images of the ice crystals-like gold nanostructure was estimated using Fractal3e analysis software employing intensity difference statistics algorithm [38].

2.6. Fabrication of the DNA biosensor

Before immobilization of p-DNA, a 10 μL of DTT solution was added to a 10 μmol L^{-1} solution of p-DNA, mixed by a vortex and placed at ambient temperature for ~30 min. Excess DTT was then extracted with an equivalent volume of ethyl acetate. A 10 μL of the resultant solution was carefully dropped onto the surface of the Au/nano electrode and kept refrigerated at 4 °C for a desired time. At this step, p-DNA self-assembling on the Au/nano electrode surface was occurred, and a p-DNA monolayer was formed by thiol-gold covalent bonds. No further layers (rather than a monolayer) were formed, because it needed attachment of further p-DNA on the pre-formed p-DNA layer on the electrode surface. In the next step and after rinsing with redistilled water, the electrode was immersed into 1.0 mmol L^{-1} 6-mercapto-1-hexanol for 30 min. Self-assembled monolayer formed upon p-DNA immobilization may contain pinholes, limbered p-DNA, defects etc. 6-mercapto-1-hexanol immobilization caused to filling the remaining gold sites and caused to form a well-aligned p-DNA monolayer. The obtained electrode is denoted as DNA biosensor throughout the text.

To optimize the immobilization time of p-DNA, open-circuit potential (OCP) measurements were performed using gold screen-printed electrodes from DropSens (Spain) covered by the ice crystals-like gold nanostructure. A 10 μmol L^{-1} solution of p-DNA was carefully dropped onto the surface of the electrodes and kept refrigerated at 4 °C for 14 h while OCP was continuously measured by a digital multimeter of Mastech Inc. (China).

2.7. *Evaluation of the DNA biosensor*

The binding time of TB with the DNA was optimized by immersing the biosensor in the TB solution during different binding times of 2, 5, 7, 10 and 15 min. Then the

biosensor was rinsed with redistilled water. Consequently, the DNA biosensor was placed in Tris and DPVs were recorded for the reduction of the bound TB.

To optimize the hybridization time of the immobilized p-DNA with c-DNA, DPVs were recorded before and after hybridization with a concentration of 1.0×10^{-10} mol L^{-1} c-DNA at different hybridization times of 10, 20, 30, 40, 50, 60, 70 and 80 min at 37 °C.

For the hybridization detection and recording readout signals, the DNA biosensor was incubated in c-DNA solutions with different concentrations of 1.0×10^{-17} to 1.0×10^{-10} mol L^{-1} at 37 °C at an intended time. The biosensor was then rinsed thoroughly with redistilled water, placed in the TB solution for 5 min, rinsed again with redistilled water, placed in Tris, and DPVs were recorded.

In order to investigate the reproducibility, the DNA biosensor was dipped into the Piranha solution for 30 s, and then re-fabricated. This procedure was repeated five times and DPVs for the repeated fabrication processes were recorded.

To study the regeneration, the DNA biosensor was hybridized with a 1.0×10^{-12} mol L^{-1} c-DNA solution. Next, it was placed into hot water at 95 °C for 5 min to de-hybridize the formed double stranded DNA (dsDNA). Then, the DNA biosensor was re-hybridized with the same c-DNA concentration. This process was repeated five times and DPVs were recorded for every step.

To inspect the stability of the DNA biosensor, DPVs for a 1.0×10^{-13} mol L^{-1} c-DNA solution was monitored at regular interval times, whereas every day after taking a DPV, the DNA biosensor was placed back into the refrigerated Tris at 4 °C.

Standard genome assays were fully validated before the clinical samples were analyzed. Standard genome samples in a range of 100 to 160 ng μL^{-1} were firstly placed at 95 °C for 5 min to de-hybridize. Then, the DNA biosensor was hybridized

with these genome samples, the corresponding signals were recorded and a calibration curve was plotted to evaluate the detection ability of EF genomic DNA by the DNA biosensor.

In order to inspect the selectivity of the DNA biosensor, synthetic sequences with base mismatches as well as a nc-DNA with a concentration of 1.0×10^{-12} mol L^{-1} were evaluated and compared with c-DNA.

2.8. Patient samples analysis

DNA analysis in clinical samples was carried out to confirm the applicability of the DNA biosensor in clinical matrices of urine and stool. All the clinical samples were collected for duration of 4 month (October 2016 through January 2017) at the Namazi hospital (Iran). The clinical specimens were submitted for a routine microbiological examination (cell culture) which among them 7 samples were found to be positive and employed for enterococci detection. The species of the bacteria in these samples were determined by PCR followed by gel electrophoresis assay (vide infra). Five samples were found to contain EF, whereas the other two samples contained *Enterococcus faecium*. Then, the genomic DNA was extracted from the samples using a commercially available kit from CinnaGen (Iran). The lysis of the bacteria and DNA extraction and purification were performed according to the kit manufacturer instructions. The DNA concentration of the samples was then determined by the NanoDrop™ Lite Spectrophotometer, and the samples were then diluted afterward. All the samples were kept in microtubes and used directly without any pretreatment.

2.9. PCR details

PCR was performed to determine the species of the bacterial in clinical samples. 1 µL of each sample was transferred to the PCR master mixture consisting 2.5 µL of 10X PCR buffer, 0.5 µL of a deoxynucleoside triphosphate mixture, 0.5 µL of each primer, 0.2 µL (5.0 U) of Taq DNA polymerase, and 0.75 µL of $MgCl_2$, and the remaining volume was filled with distilled water. Amplification was consisted of an initial denaturation at 95 °C for 5 min, followed by 30 cycles of 30 s at 95 °C, 30 s at 61 °C, and 45 s at 72 °C.

2.10. Gel electrophoresis

The PCR products were detected by 2% agarose gel electrophoresis with 1X TEA (Tris EDTA acetate) as a running buffer. Gel was incubated with 1 µL of a DNA safe stain from CinnaGen (Iran) and was polymerized for 40 min at room temperature. A volume of 7 µL of each sample was mixed with 1 µL of the loading buffer and was subjected to gel electrophoresis. After electrophoresis, the fragments were visualized under UV light in a gel documentation system.

3. Results and discussion

FESEM images at different magnification and an energy-dispersive X-ray spectrum of the electrodeposited gold nanostructure are shown in Fig. 1. The gold nanostructure resembled to ice crystals with triangular blades with spaces at the bottom providing a highly rough surface. Each crystal consists of smaller attached triangle particles. The energy-dispersive X-ray spectrum confirms the chemical purity of the electrodeposited structure. The surface of the gold nanostructure can be characterized by a fractal dimension which indicates the scaling performance of surface roughness. It also estimates the surface fragment and irregularity. The fractal

dimension of the gold nanostructure was obtained as 2.44±0.19 from the FESEM images, indicating irregularity and fragmentation of the nanostructure to a certain extent. This synthesized gold nanostructure provides an appropriate substrate for p-DNA immobilization and hence may result in improved detection of hybridization process. Therefore, it is expected that the nanostructure can amplify the electrochemical signal, which in turn lead to a biosensor with higher sensitivity and specificity [7-14]. The real surface area of the gold nanostructure (A_r) was also electrochemically obtained to be 0.30 cm^2 (Supporting information S1), indicating a roughness factor (rugosity, equal to A_r/A_g, where A_g is the geometric surface area) of 9.5 for the Au/nano electrode. Therefore, the ice crystals-like gold nanostructure provided a high surface area substrate for the immobilization of p-DNA.

TB is a phenothiazine dye exhibiting a redox transition as:

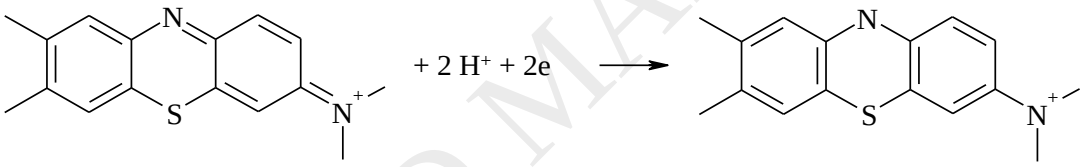

Interaction of TB with DNA has been investigated using different methods [39-41]. However, discrimination of the single stranded DNA (ssDNA) from dsDNA by TB and its application for detection of hybridization event has been rarely approached. Fig. 2 shows cyclic voltammograms of the Au electrode as well as the DNA biosensor before and after hybridization with 1.0×10^{-13} mol L^{-1} c-DNA in a solution of 20 μmol L^{-1} TB dissolved in Tris. TB displays a pair of quasi-reversible redox peaks at a formal potential (as a mead peak) of ~-290 mV. The TB formal potential shifts to ~-278 mV in the presence of p-DNA at the electrode surface, indicating a hydrophobic interaction between TB and p-DNA [42, 43]. Upon formation of dsDNA at the biosensor surface through hybridization of TB with c-

DNA, the formal potential shifts to ~-264 mV. This positive potential shift further confirms the binding of TB with the dsDNA structure via hydrophobic attractions at the concentration range employed in this study. Higher positive shift in the formal potential of TB as a result of binding with dsDNA can be an indicator for stronger attraction between TB and dsDNA. Meanwhile, it has been reported that TB intercalates into the DNA base pairs at low concentrations, whereas it attaches to the negatively charged phosphate groups at higher concentrations [44]. It can be concluded thus that TB binds with dsDNA in a higher extent compared to ssDNA. The peak current can therefore be employed to discriminate between ssDNA and dsDNA structures at the electrode surface. The decrement in the peak current of TB interacted with dsDNA can be also related to both the effect of stronger binding of TB with dsDNA (compared to ssDNA), and/or lower concentration of the bonded TB to DNA. Based on presented hypothesis, it can be concluded that TB more strongly bind to dsDNA. This binding suppresses the electron exchange between TB and underlying surface. Accordingly, the peak currents in the voltammogram shown in Fig. 2 recorded using the DNA biosensor decreases after binding with c-DNA compared to that of without c-DNA binding. Therefore, TB was employed as the redox hybridization marker for fabrication of the DNA biosensor. In the following, however, DPVs were measured for the reduction of bound TB into the biosensor to evaluate its performance because differential pulse voltammetry is more sensitive than cyclic voltammetry, and the reduction peak current of TB is greater than the oxidation one.

In order to obtain a high detection sensitivity and improve its detection efficiency, different experimental parameters were optimized for the DNA biosensor. The time of p-DNA immobilization on the Au/nano electrode surface was firstly investigated during more than 9 h. It was observed (Supporting information S2) that with

increasing the immobilization time, OCP regularly changed and reached a steady value after ~350 min. Accordingly, an immobilization time of 6 h was selected for the fabrication of the DNA biosensor. The best binding time of TB with the DNA biosensor was also evaluated and the corresponding DPVs were recorded (Fig. 3A). The peak current increased during the first 5 min and maintained a plateau level at afterward. Thus, 5 min was selected as the best TB binding time. To optimize the hybridization time of c-DNA with the biosensor, DPVs were recorded using the biosensor fabricated at different hybridization times with 1.0×10^{-10} mol L^{-1} c-DNA (Fig. 3B). The peak current decreased during the first 60 min hybridization time and remained unchanged thereafter due to the saturated hybridization between c-DNA and p-DNA. Therefore, 60 min was selected as the best hybridization time.

Fig. 4A shows DPVs recorded using the DNA biosensor upon hybridization with different concentrations of c-DNA. With increment in the c-DNA concentration, the immobilized p-DNA at the surface captures more c-DNA and consequently the peak current caused by the reduction of the redox marker decreases. A calibration curve was ploted based on the dependency of the peak current on the c-DNA concentration which is presented in Fig. 4B. The calibration curve displays a regression equation of $y = -(0.466\pm0.012) \log C_{c\text{-}DNA} - (0.117\pm0.164)$ with a regression coefficient of 0.9961 in a concentration range of 1.0×10^{-17} to 1.0×10^{-10} mol L^{-1} of c-DNA. The limit of detection (LOD) was calculated as 3σ using the regression equation based on the standard deviation (σ) of the blank signal (peak current in the absence of c-DNA) to be 4.7×10^{-20} mol L^{-1} for c-DNA detection. The LOD obtained using the prepared biosensor is much lower than the reported values in literature. A comparison between different EF detection methods is presented in Table 1. The DNA biosensor presented in this study demonstrated the best detection performance, compared to the other

reported methods. Fabrication of the DNA biosensor and c-DNA detection is presented in Scheme 1.

Reproducibility, regeneration and stability are extremely important features for a biosensor in practical applications. The reproducibility of the DNA biosensor fabrication was explored by measuring the relative standard deviation (RSD) for the peak current (Supporting information S3). The obtained RSD value of 3.7% indicates that the DNA biosensor exhibits an excellent reproducibility for target determination. To evaluate the regeneration, the DNA biosensor were subjected to 5 cycles of hybridization/dehybridization and corresponding responses were measured after (Supporting information S4). The difference between the current responses after hybridization/dehybridization showed a RSD value of 4.8%. Stability of the DNA biosensor was also examined by monitoring the changes in the peak currents of DPVs for the DNA biosensor after hybridization with 1.0×10^{-13} mol L^{-1} of c-DNA during several days (Supporting information S5). The biosensor signal was disappeared within ~27 days which can be considered as the stability time.

In order to apply the DNA biosensor for EF genome detection, the genome was extracted and DNA concentration was determined. A stock solution of genome was prepared and analysis was performed for the prepared serial dilution. DPVs were recorded using the DNA biosensor upon hybridization with different concentrations of the genome as shown in Fig. 5A. The corresponding calibration curve is also plotted and shown in Fig. 5B. The calibration curve demonstrate a regression equation of $y = -(13.90\pm0.47) \log C_{DNA} + (36.68\pm1.00)$ with a regression coefficient of 0.9965. LOD was obtained based on the standard deviation of the blank signal and the regression equation to be 30.1 ng μL^{-1} for detection of genomic DNA. The LOD obtained here is

much lower compared to the other reported methods (Table 1), indicating the higher sensitivity of the prepared DNA biosensor.

One of the greatest challenges facing the development of DNA biosensors is their ability to recognize the similar DNA sequences. The selectivity test was achieved by hybridization of the prepared DNA biosensor with ssDNA sequences having base mismatched. Supporting information S6 shows DPVs recorded using the DNA biosensor upon hybridization with c-DNA, 1miss-DNA, 2miss-DNA, 3miss-DNA and nc-DNA with a concentration of 1.0×10^{-12} mol L^{-1}. The decrement in the peak current was the highest for c-DNA among the four sequences due to the effective and complete hybridization, while this decrement depends on the level of the base mismatches. The results indicates that the prepared DNA biosensor is selective towards c-DNA.

Since the detection ability of the DNA biosensors may be influenced in the complex matrices of the real samples, the DNA biosensor was applied for the detection of the pathogen in human specimens. In a typical experiment, genome was extracted from the human samples. A part of the extracted genomic DNA samples was firstly amplified by PCR and then analyzed by gel electrophoresis to identify the bacterium species in the human samples. The other part of the genomic DNA samples was directly analyzed by the DNA biosensor. Initially, the peak currents related to the DNA biosensor were recorded in the absence of any samples in ten replicates. Then, DPVs were recorded for the human samples and the corresponding peak currents were measured. The positive samples were determined by measuring the decrement in the peak current, considering 10σ as the threshold value. The samples with the increments greater than 10σ were indicated as the positive. The obtained results are also summarized in Supporting information S7. The comparison of the obtained analysis

results from the DNA biosensor with the standard method indicates that the DNA biosensor can be successfully employed in analysis of the clinical samples.

4. Conclusion

In summary, an electrodeposition method was developed to fabricate a new gold nanostructure. The obtained nanostructure was characterized indicating it owed a high surface area and roughness factor. After immobilization of a thiolated EF-specific DNA probe, this high surface area of the crystals-like gold nanostructure provided a high surface concentration of the probe and a highly sensitive DNA biosensor. Hybridization of the immobilized probe with a variety of sequences, including c-DNA, 1miss-DNA, 2miss-DNA, 3miss-DNA, nc-DNA and EF genomic DNA was monitored using TB as a novel redox hybridization marker at optimized experimental parameters. The developed biosensor represented excellent sensitivity and selectivity with a low detection limit. The developed biosensor can be employed as an alternative method for EF detection without using PCR amplification in clinical samples for positive/negative diagnosis.

Acknowledgments

Research reported in this publication was supported by Elite Researcher Grant Committee under award number [943601] from the National Institutes for Medical Research Development (NIMAD), Tehran, Iran. We would also like to thank the Research Consultation Center of Shiraz University of Medical Sciences.

References

[1] S.M. Yoo, S.Y. Lee, Optical biosensors for the detection of pathogenic microorganisms, Trends Biotechnol. 34 (2016) 7-25.

[2] Y. Amano, Q. Cheng, Detection of influenza virus:Traditional approaches and development of biosensors, Anal. Bioanal. Chem. 381 (2005) 156-164.

[3] N. Sattarahmady, H. Heli, R.D. Vais, An electrochemical acetylcholine sensor based on lichen-like nickel oxide nanostructure, Biosens. Bioelectron. 48 (2013) 197-202.

[4] N. Sattarahmady, A. Movahedpour, H. Heli, G.R. Hatam, Gold nanoparticles-based biosensing of *Leishmania major* kDNA genome: Visual and spectrophotometric detections, Sens. Actuat. B 235 (2016) 723-731.

[5] H. Heli, M. Hajjizadeh, A. Jabbari, A.A. Moosavi-Movahedi, Copper nanoparticles-modified carbon paste transducer as a biosensor for determination of acetylcholine, Biosens. Bioelectron. 24 (2009) 2328-2333.

[6] N. Sattarahmady, Z. Kayani, H. Heli, Highly simple and visual colorimetric detection of *Brucella* melitensis genomic DNA in clinical samples based on gold nanoparticles, J. Iran. Chem. Soc. 12 (2015) 1569-1576.

[7] J. Mohammadi, A. Moattari, N. Sattarahmady, N. Pirbonyeh, H. Yadegari, H. Heli, Electrochemical biosensing of influenza A subtype genome based on meso/macroporous cobalt (II) oxide nanoflakes-applied to human samples. Anal. Chim. Acta. 979 (2017) 51-57.

[8] A. Rahi, N. Sattarahmady, H. Heli, An ultrasensitive electrochemical genosensor for *Brucella* based on palladium nanoparticles, Anal Biochem. 510 (2016) 11-17.

[9] M. Moradi, N. Sattarahmady, G.R. Hatam, H. Heli, Electrochemical genosensing of *Leishmania major* using gold hierarchical nanoleaflets, J. Biol. Today's World, 5 (2016) 128-136.

[10] H. Heli, N. Sattarahmady, G.R. Hatam, F. Reisi, R.D. Vais, An electrochemical genosensor for *Leishmania major* detection based on dual effect of immobilization and electrocatalysis of cobalt-zinc ferrite quantum dots, Talanta 156-157 (2016) 172-179.

[11] M. Negahdary, M. Behjati-Ardakani, N. Sattarahmady, H. Yadegari, H. Heli, Electrochemical aptasensing of human cardiac troponin I based on an array of gold nanodumbbells-Applied to early detection of myocardial infarction, Sens. Actuat. B 252 (2017) 62-71.

[12] A. Rahi, N. Sattarahmady, H. Heli, Label-free electrochemical aptasensing of the human prostate-specific antigen using gold nanospears, Talanta 156 (2016) 218-224.

[13] A. Rahi, N. Sattarahmady, H. Heli, Zepto-molar electrochemical detection of Brucella genome based on gold nanoribbons covered by gold nanoblooms, Sci. Rep. 5 (2015) Article number 18060.

[14] N. Sattarahmady, A. Rahi, H. Heli, A signal-on built in-marker electrochemical aptasensor for human prostate-specific antigen based on a hairbrush-like gold nanostructure. Sci. Rep. 7 (2017) Article number 11238.

[15] J. Castillo, S. Gaspar, S. Leth, M. Niculescu, A. Mortari, I. Bontidean, I. Bontidean, V. Soukharev, S. A. Dorneanu, A. D. Ryabov, E. Csoregi, Biosensors for life quality: Design, development and applications, Sens. Actuat. B 102 (2004) 179-194.

[16] L.M. Teixeira, V.L.C. Merquior, Enterococcus, Molecular Typing in Bacterial Infections, Springer, 2013, 17-26.

[17] Y. Cai, H. Pang, M. Kitahara, M. Ohkuma, Lactobacillus nasuensis sp. nov., a lactic acid bacterium isolated from silage, and emended description of the genus Lactobacillus, Int. J. Syst. Evol. Microbiol. 62 (2012) 1140-1144.

[18] M.S. Endo, F.G.C. Signoretti, V.S. Kitayama, A.C.S. Marinho, F.C. Martinho, B.B.P.F. de Almeida, B. B. P. de Almeida, G. Gomes, Investigation in vivo of Enterococcus faecalis in endodontic retreatment by phenotypic and genotypic methods, Acta Scientiarum Health Sci. 37 (2015) 95-103.

[19] M.R. Cruz, C.E. Graham, B.C. Gagliano, M.C. Lorenz, D.A. Garsin, *Enterococcus faecalis* inhibits hyphal morphogenesis and virulence of *Candida albicans*, Infect. Immun. 81 (2013) 189-200

[20] C.M. Sedgley, A.C. Nagel, C.E. Shelburne, D.B. Clewell, O. Appelbe, A. Molander, Quantitative real-time PCR detection of oral *Enterococcus faecalis* in humans, Arch. Oral Biol. 50 (2005) 575-583.

[21] M.M. Huycke, C.A. Spiegel, M.S. Gilmore, Bacteremia caused by hemolytic, high-level gentamicin-resistant *Enterococcus faecalis*, Antimicrob. Agents Chemother. 35 (1991) 1626-1634.

[22] K. Fisher, C. Phillips, The ecology, epidemiology and virulence of Enterococcus, Microbiol. 155 (2009) 1749-1757.

[23] Y. Wang, E.C. Alocilja, Gold nanoparticle-labeled biosensor for rapid and sensitive detection of bacterial pathogens, J. Biol. Eng. 9 (2015) 1-7.

[24] Y. Hu, X. Xu, Q. Liu, L. Wang, Z. Lin, G. Chen, Ultrasensitive electrochemical biosensor for detection of DNA from Bacillus subtilis by coupling target-Induced

strand displacement and nicking endonuclease signal amplification, Anal. Chem. 86 (2014) 8785-8790.

[25] X. Ma, Y. Jiang, F. Jia, Y. Yu, J. Chen, Z. Wang, An aptamer-based electrochemical biosensor for the detection of Salmonella, J. Microbiol. Methods 98 (2014) 94-98.

[26] N. Sattarahmady, G.H. Tondro, M. Golchin, H. Heli, Gold nanoparticles biosensor of *Brucella* spp. genomic DNA: Visual and spectrophotometric detections, Biochem. Eng. J. 97 (2015) 1-7.

[27] A. Subramanian, J. Irudayaraj, T. Ryan, A mixed self-assembled monolayer-based surface plasmon immunosensor for detection of E. coli O157: H7, Biosens. Bioelectron. 21 (2006) 998-1006.

[28] H. Mukundan, S. Kumar, D.N. Price, S.M. Ray, Y.-J. Lee, S. Min, Ye-J Lee, S. Min, S. Eum, J. Kubicek-Sutherland, J. Resnick, W. K. Grace, Rapid detection of Mycobacterium tuberculosis biomarkers in a sandwich immunoassay format using a waveguide-based optical biosensor, Tuberculosis 92 (2012) 407-416.

[29] Z. Wang, P. Han, X. Mao, Y. Yin, Y. Cao, Sensitive detection of glutathione by using DNA-templated copper nanoparticles as electrochemical reporters, Sens. Actuat. B 238 (2017) 325-330.

[30] P. Yanez-Sedenno, L. Agui, R. Villalonga, J.M. Pingarron, Biosensors in forensic analysis. A review, Anal. Chim. Acta 823 (2014) 1-19.

[31] S. Scarano, E. Dausse, F. Crispo, J.J. Toulme, M. Minunni, Design of a dual aptamer-based recognition strategy for human matrix metalloproteinase 9 protein by piezoelectric biosensors, Anal. Chim. Acta 897 (2015) 1-9.

[32] J. Wang, G. Rivas, J.R. Fernandes, J.L.L. Paz, M. Jiang, R. Waymire, Indicator-free electrochemical DNA hybridization biosensor, Anal. Chim. Acta 375 (1998) 197-203.

[33] Y. Wang, H. Li, Y. Wang, L. Zhang, J. Xu, C. Ye, Loop-mediated isothermal amplification label-based gold nanoparticles lateral flow biosensor for detection of Enterococcus faecalis and Staphylococcus aureus, Front. Microbiol. 8 (2017) 192.

[34] S.L. La Rosa, M. Solheim, D.B. Diep, I.F. Nes, D.A. Brede, Bioluminescence based biosensors for quantitative detection of enterococcal peptide-pheromone activity reveal inter-strain telesensing in vivo during polymicrobial systemic infection, Sci. Rep. 5 (2015) Article number 8339.

[35] J.L. de Miranda, M.D. Oliveira, I.S. Oliveira, I.A. Frias, O.L. Franco, C.A. Andrade, A simple nanostructured biosensor based on clavanin A antimicrobial peptide for gram-negative bacteria detection, Biochem. Eng. J. 124 (2017) 108-114.

[36] A.J. Bard, L.R. Faulkner, Electrochemical Methods, Wiley, New York, 2001.

[37] S.F. Wang, Q. Xu, Electrochemical parameters of ethamsylate at multi walledcarbon nanotube modified glassy carbon electrodes, Bioelectrochemistry 70(2007) 296-300.

[38] E.L. Land, S. Hiroyuki, J. Tochigi, Fractal analysis system for windows, National Institute of Livestock and Grass-land Sci. Nishinasuno, 2006.

[39] P. Paul, G. Suresh Kumar, Spectroscopic studies on the binding interaction of phenothiazinium dyes toluidine blue O, azure A and azure B to DNA, Spectrochim. Acta A 107 (2013) 303-310.

[40] K. Jiao, Q.J. Li, W. Sun, Z.J. Wang, Voltammetric detection of the DNA interaction with toluidine blue, Electroanalysis 17 (2005) 997-1002.

[41] M. Ilanchelian, R. Ramaraj, Binding interactions of toluidine blue O with Escherichia coli DNA: Formation of bridged structure, J. Fluoresc. 21 (2011) 1439-1453.

[42] H. Heli, N. Sattarahmady, A. Jabbari, A.A. Moosavi-Movahedi, G.H. Hakimelahi, F.-Y. Tsai, Adsorption of human serum albumin onto glassy carbon surface-Applied to albumin-modified electrode: Mode of protein-ligand interactions, J. Electroanal. Chem. 610 (2007) 67-74.

[43] H. Heli, A.A. Moosavi-Movahedi, A. Jabbari, F. Ahmad, An electrochemical study of safranin O binding to DNA at the surface, J. Solid State Electrochem. 11 (2007) 593-599.

[44] Z. Chi, R. Liu, Y. Sun, M. Wang, P. Zhang, C. Gao, Investigation on the toxic interaction of toluidine blue with calf thymus DNA, J. Hazard. Mater. 175 (2010) 274-278.

[45] R.A. Haugland, S.C. Siefring, L.J. Wymer, K.P. Brenner, A.P. Dufour, Comparison of Enterococcus measurements in freshwater at two recreational beaches by quantitative polymerase chain reaction and membrane filter culture analysis, Water. Res. 39 (2005) 559-568.

[46] J.-W. He, S. Jiang, Quantification of enterococci and human adenoviruses in environmental samples by real-time PCR, Appl. Environ. Microbiol. 71 (2005) 2250-2255.

[47] G.O. Zoletti, J.F. Siqueira, K.R.N. Santos, Identification of *Enterococcus faecalis* in root-filled teeth with or without periradicular lesions by culture-dependent and-independent approaches, J. Endod. 32 (2006) 722-726.

[48] K. Waar, J.E. Degener, M.J. van Luyn, H.J.M. Harmsen, Fluorescent in situ hybridization with specific DNA probes offers adequate detection of Enterococcus faecalis and Enterococcus faecium in clinical samples, J. Med. Microbiol. 54 (2005) 937-944.

[49] D.-K. Kim, S.M. Yoo, T.J. Park, H. Yoshikawa, E. Tamiya, J.Y. Park, S. Y. Lee, Plasmonic properties of the multispot copper-capped nanoparticle array chip and its application to optical biosensors for pathogen detection of multiplex DNAs, Anal. Chem. 83 (2011) 6215-6222.

Figure legends

Fig. 1: FESEM images (A-D) at different magnification and an energy-dispersive X-ray spectrum (E) of the electrodeposited gold nanostructure.

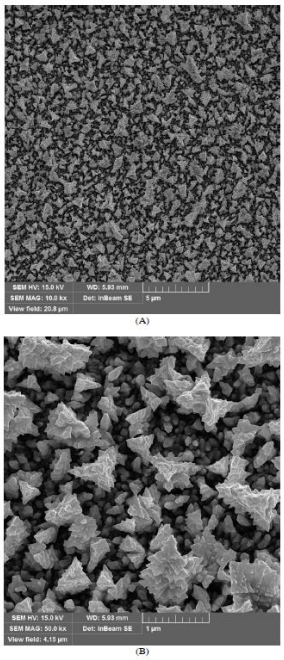

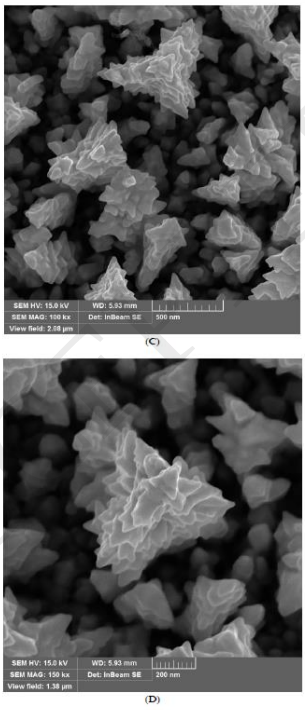

Fig. 2: Cyclic voltammograms of the Au electrode, and the DNA biosensor before and after hybridization with 1.0×10^{-13} mol L^{-1} c-DNA in a solution of 20 µmol L^{-1} TB dissolved in Tris. The potential sweep rate was 50 mV s^{-1}.

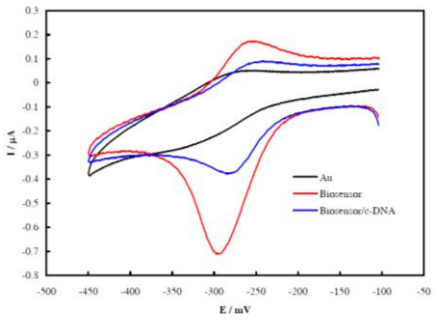

Fig. 3: DPVs recorded using the DNA biosensor after binding with 20 µmol L^{-1} TB in Tris after different binding times of 2, 5, 7, 10 and 15 min (A). DPVs recorded using the DNA biosensor before and after hybridization at 37 °C with 1.0×10^{-10} mol L^{-1} c-DNA at different hybridization times of 10, 20, 30, 40, 50, 60, 70 and 80 min (B).

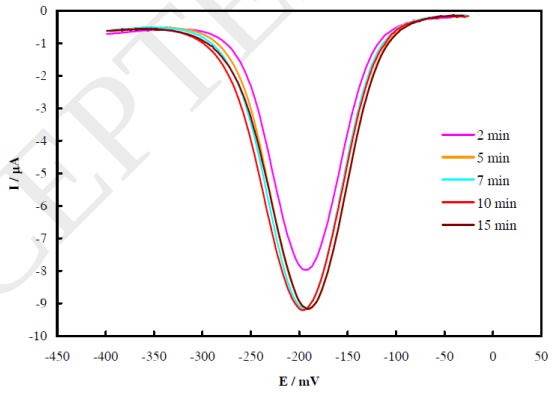

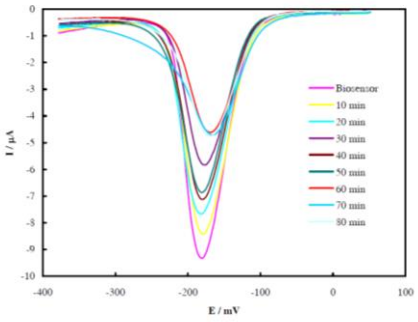

Fig. 4: DPVs recorded using the DNA biosensor upon hybridization with different concentrations of c-DNA (A), and the corresponding calibration curve (B).

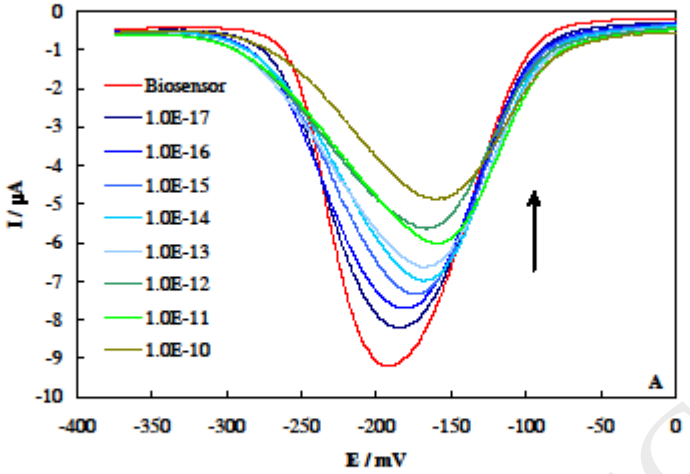

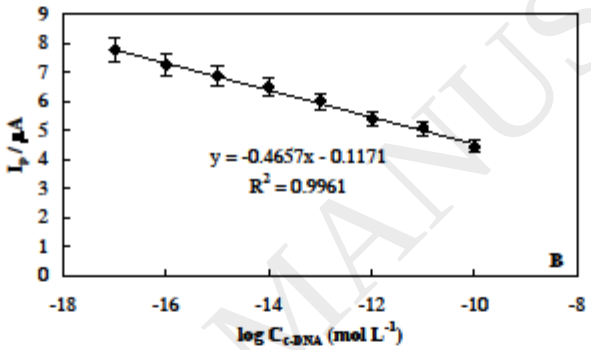

Fig. 5: DPVs recorded using the DNA biosensor upon hybridization with different concentrations of genomic DNA (A), and the corresponding calibration curve (B).

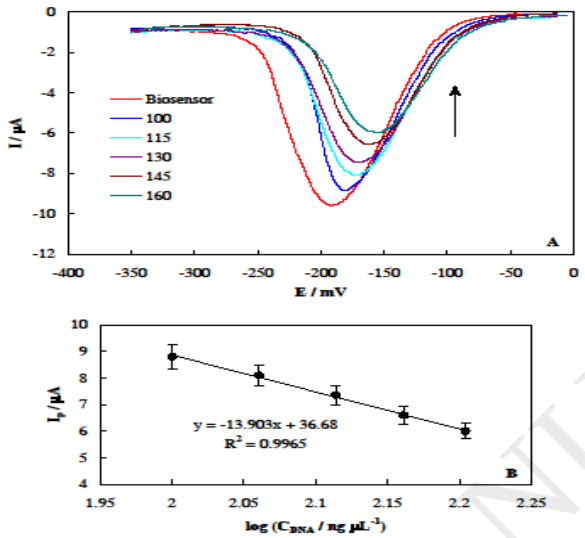

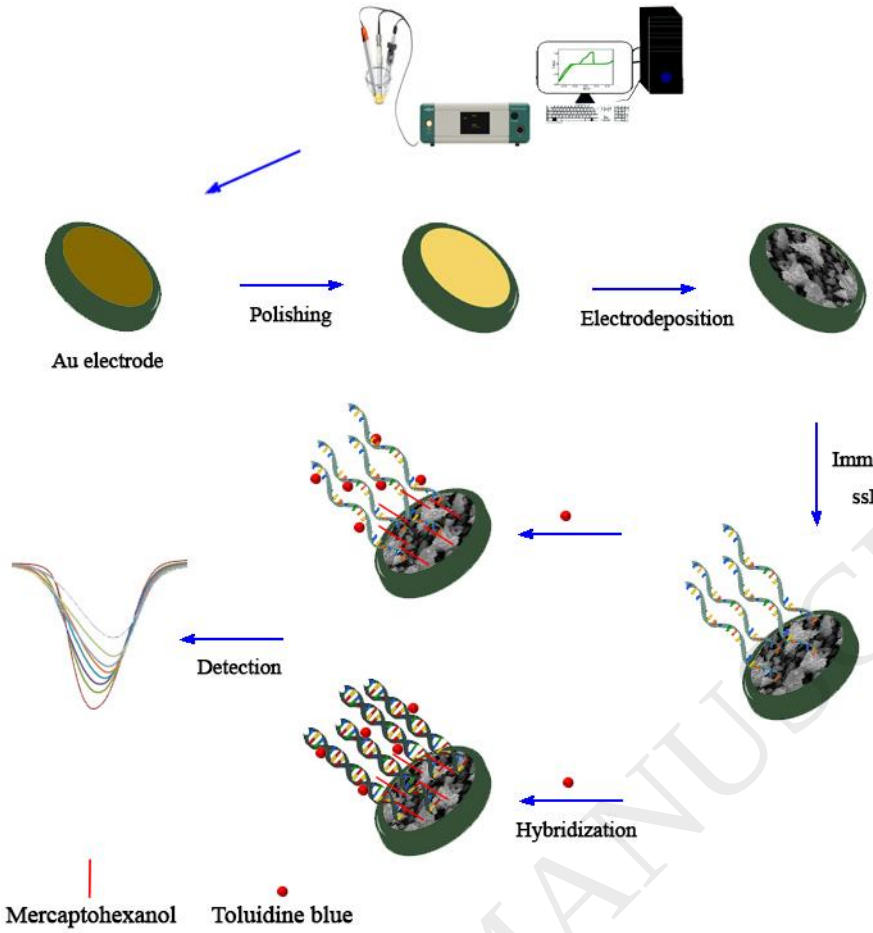

SCHEME 1

Table 1: A comparison between different methods of EF detection.

Method detection	LOD or LOQ*	Reference
Culture assays	7%**	[20]
LAMP	250 fg per reaction	[33]
Bioluminescence-based reporter	640 CIU***	[34]
Clavanin A peptide and cysteine-gold nanoparticles-based biosensor	10 CFU	[35]
Quantitative PCR	3 CFU	[45]
Membrane filtering	1 CFU	[45]
Real-time PCR	5 CFU/reaction	[46]
PCR	80%	[47]
Culture assays	16%	[47]
Fluorescent in situ hybridization	10^7 cells	[48]
Localized surface plasmon resonance	10 fmol L^{-1}	[49]
DNA biosensor	4.7×10^{-20} mol L^{-1} (c-DNA)	This work
DNA biosensor	30.1 ng μL^{-1} (genome)	This work

* LOQ: Limit of quantitation

** Percent indicates the identified cases over all of the samples.

*** CIU: Cytolysin small subunit-Inducing Units